



Optimization of electrochemical decolorization of certain arylazo pyridone dyes

JELENA M. MIRKOVIĆ[#], NEVENA Ž. PRLAINOVIĆ[#], GORDANA S. UŠĆUMLIĆ[#],
BRANIMIR N. GRGUR and DUŠAN Ž. MIJIN*[#]

Faculty of Technology and Metallurgy, University of Belgrade, Kneževićevo 4,
11020 Belgrade, Serbia

(Received 9 April, revised 30 May 2014, accepted 18 June 2014)

Abstract: Electrocatalytic decolorization of arylazo pyridone dyes was investigated in the presence of sodium chloride using a DSA Ti/PtO_x electrode in dilute sodium hydroxide. The decolorization could be attributed to the indirect oxidation of the investigated dyes by electrogenerated hypochlorite formed from the chloride oxidation. The electrochemical decolorization was investigated for the different sodium hydroxide concentrations in the range from 40 mg dm⁻³ to 4 g dm⁻³, sodium chloride concentrations in the range from 15 to 40 g dm⁻³, currents in the range of 100 to 250 mA and dye concentrations from 5 to 20 mg dm⁻³. The optimum electrolysis conditions are suggested. The effect of substituents on the reaction rate was also studied.

Keywords: pyridone; electrolysis; hypochlorite; UV–Vis spectroscopy; donor–acceptor effects.

INTRODUCTION

Arylazo pyridone dyes have become important in the last several decades due to their high molar extinction coefficients and medium to high light and wash fastness properties.¹ These dyes generally find application as disperse dyes and are used for the dyeing of hydrophobic fibers (polyesters and nylons as the main synthetic fibers). Furthermore, disperse dyes have been employed in the inks for the heat-transfer printing of polyesters.²

Synthetic azo dyes are pollutants that represent a significant source of environmental contamination. Due to the presence of an azo group, they are not easily degradable. Most of the physico-chemical methods, such as chemical precipitation and separation of pollutants, coagulation, elimination by adsorption, etc.,

* Corresponding author. E-mail: kavur@tmf.bg.ac.rs

[#] Serbian Chemical Society member.

doi: 10.2298/JSC140409063M

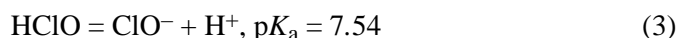
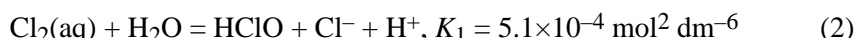
do not degrade dye molecules but only transfer the contamination from one phase to another, causing a new kind of pollution.^{3–5}

Photodegradation, ozonation, alkalinization, and electrochemical methods are some of the methods that could be used for the decolorization or the degradation of the dyes.^{5,6} Indirect oxidation, based on the homogeneous reaction between anodically generated oxidizing species and dyes, is the most favorable of the electrochemical methods. The addition of an electrolyte is necessary in order to obtain better fixation and exhaustion during the dyeing process with reactive and direct or substantive dyes. An amount of 50–80 g dm⁻³ of a salt is generally added as an electrolyte, most commonly sodium chloride or sodium sulfate.⁷ Since it is not necessary to add any salt during the dyeing process when disperse dyes are used, some salt should be introduced into the wastewater before the electrochemical treatment. Sodium chloride is one of the best solutions. During the electrolysis, depending on the conditions, strong oxidizing species – chlorine, hypochlorous acid or hypochlorite, are formed on the anode. At higher pH, *e.g.*, pH > 6, hypochlorous acid can dissociate to form hypochlorite and H⁺. At pH lower than 3.5, hypochlorous acid yields Cl₂. Mixtures of these species are usually named “active chlorine”.^{7,8}

During electrolytic hypochlorite production, the oxidation of the chloride to solvated chlorine occurs first at the anode surface:



followed by the secondary solution phase reactions:^{7,8}



Arylazo pyridone dyes were already subjected to photolysis and photocatalysis. The photofading kinetics of 3-(*p*- and *o*-substituted arylazo)-5-cyano-2-hydroxy-4-methyl-6-pyridone dyes in amide solvents (*N,N*-dimethylformamide, formamide, and *N,N*-dimethylacetamide) and *n*-hexane were previously studied. It was established that the photofading rate increases with increasing solvation of the dyes, as well as in the presence of two electron-withdrawing substituents (NO₂ and Cl) on the benzene ring.⁹ The same authors also studied the photo-stability of 3-(mono- and di-substituted arylazo)-5-cyano-2-hydroxy-4-methyl-6-pyridones in *N,N*-dimethylformamide under 254 nm light. It was found that the simultaneous presence of two electron-withdrawing substituents in the diazo component of the dyes caused an increase in the fading rate, while the introduction of an hydroxyalkyl group to the coupling component resulted in a decrease in the fading rate.¹⁰ In addition, the arylazo pyridone dyes were applied to polyester fabrics and the effects of substituents on the photofading on polyester substrates was studied.^{11,12} Electron-withdrawing substituents on aniline inc-

reased the photostability and improved the sublimation fastness of azo dyes on polyesters, while the β -hydroxyethyl group increased the fading rate. Besides direct photodegradation, photocatalytic degradation of 5-(4-sulphophenylazo)-3-cyano-6-hydroxy-4-methyl-2-pyridone in the presence of commercial TiO₂ was studied in aqueous solution under simulated sunlight. Optimal conditions were established and the dye was successfully degraded.^{13,14} Arylazo pyridone dyes (Fig. 1) have not been previously solely subjected to the electrochemical treatment except as a component of a wastewater.¹⁵

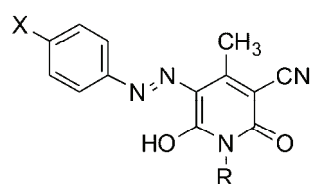


Fig. 1. Structure of the 5-arylazo-3-cyano-6-hydroxy-4-methyl-2-pyridones ($R = \text{CH}_2\text{CH}_2\text{OH}$, $X = \text{OCH}_3$ (**1**), OH (**2**), NO_2 (**3**), H (**4**), COCH_3 (**5**), CH_3 (**6**), COOH (**7**), Cl (**8**), Br (**9**), CN (**10**)); $R = \text{H}$, $X = \text{OCH}_3$ (**11**); $R = \text{CH}_2\text{CH}_3$, $X = \text{OCH}_3$ (**12**)).

The aim of the present study was to investigate the electrocatalytic decolorization of arylazo pyridone dyes in water by indirect electrochemical oxidation. The effects of different operating factors, such as agitation speed, concentration of supporting electrolyte, applied current density, initial dye concentration and solution pH, on the dye decolorization were analyzed in order to optimize the conditions of electrochemical treatment. The effect of the dye structure on the reaction rate was also studied.

EXPERIMENTAL

Materials and methods

All starting materials were obtained from Aldrich and Fluka, and were used without further purification. Sodium chloride was p.a. grade (Merck). Deionized water was obtained from a Milipore Waters Milli-Q purification unit. The IR spectra were determined using a Bomem Fourier transform-infrared (FT-IR) spectrophotometer, MB-Series in the form of KBr pellets. The ¹H- and ¹³C-NMR spectral measurements were performed on a Varian Gemini 2000 (200 MHz). The spectra were recorded at room temperature in deuterated dimethyl sulfoxide (DMSO-*d*₆). The chemical shifts are expressed in ppm values referenced to TMS. The ultraviolet-visible (UV-Vis) absorption spectra were recorded on a Schimadzu 1700 spectrophotometer in the region 200–700 nm. All melting points were determined using a Stuart SMP30 apparatus and are given in degree Celsius. Elemental analyses were performed using a Vario EL III elemental analyzer.

Preparation of arylazo pyridone dyes

The investigated arylazo pyridone dyes were synthesized from the corresponding diazonium salts and substituted 2-pyridones using classical reaction for the synthesis of the azo compounds.¹⁶ 3-Cyano-4-methyl-6-hydroxy-2-pyridone, 1-ethyl-3-cyano-6-hydroxy-4-methyl-2-pyridone and 3-cyano-6-hydroxy-1-(2-hydroxyethyl)-4-methyl-2-pyridone were prepared from cyanoacetamide or substituted cyanoacetamide and ethyl acetylacetate.^{13,17} Substituted cyanoacetamides were prepared from corresponding amine and ethyl cyanoacetate.¹⁸ Dyes **3**, **4**, **6**, **8**, **11** and **12** are described in literature.^{10–12,19–22} The physical, analytic

and spectral data for the synthesized dyes are given in the Supplementary material to this paper.

Electrochemical decolorization

Electrochemical decolorization process was investigated in a cylindrical glass electrochemical cell with an electrolyte volume of 500 cm³. The electrolyte was prepared from distilled water, NaCl and the required dye. A 5 cm² Ti/PtO_x electrode, obtained by thermal decomposition of H₂PtCl₆ in 2-propanol with 1 mg cm⁻² of platinum loading, was used as the anode, while the cathode was a 10 cm² plate made from austenite 18Cr/8Ni stainless steel series 304. The electrodes with a gap of 3 mm were immersed at the top of the electrolyte. For the electrolysis of solution, the galvanostatic mode of a PAR M273 potentiostat/galvanostat was used. Mixing of the electrolyte was accomplished by a magnetic stirrer with controlled agitation speed. During the electrolysis, at certain times, 3 cm³ of solution was removed with a micropipette and its UV–Vis spectrum was instantly recorded on a Shimadzu model 1700 spectrophotometer. This enabled the concentration of the dye to be followed during the course of its degradation.

RESULTS AND DISCUSSION

Reaction kinetics and UV–Vis spectra

Arylazo pyridone dyes, as mentioned before, are the disperse dyes characterized by low aqueous solubility. In order to study the reaction kinetics of the decolorization, an aqueous solution of the arylazo pyridone dye should be prepared first. Since these dyes are more soluble in the basic media, the influence of

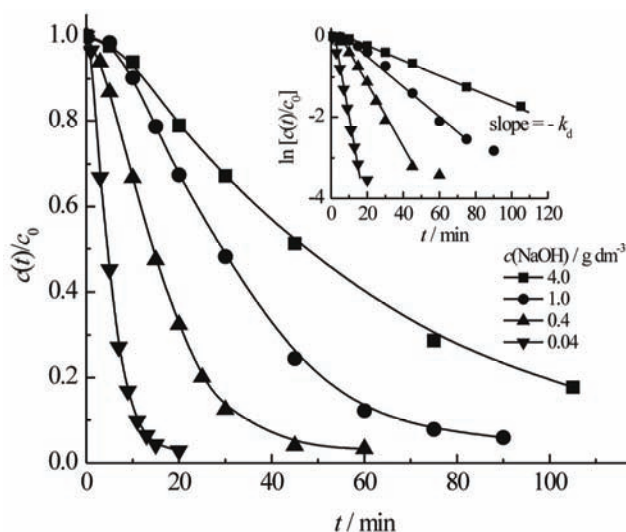


Fig. 2. Dependence of the relative dye **1** concentration over time for different sodium hydroxide concentration (marked in the figure). Insert: the logarithmic plot of the relative concentration of dye *vs.* electrolysis time for different sodium hydroxide concentrations.

Conditions: $c(\text{dye } \mathbf{1}) = 10 \text{ mg dm}^{-3}$ (30.4 μM), $c(\text{NaCl}) = 20 \text{ g dm}^{-3}$, $\omega = 250 \text{ rpm}$, $I = 200 \text{ mA}$.

sodium hydroxide concentration was studied and the results are given in Fig. 2. To increase solubility, dyes from 3-cyano-6-hydroxy-1-(2-hydroxyethyl)-4-methyl-2-pyridone were synthesized and dye **1** was used as a model compound to study the effect of the sodium hydroxide concentration on the reaction rate of the decolorization. The sodium hydroxide concentration was varied between 4 g dm⁻³ (0.1 M) to 40 mg dm⁻³ (1 mM). The initial sodium chloride concentration and the applied current value were taken according to the results in a previous paper.²³ During the electrochemical treatment, at certain times, 3 cm³ of reaction solution was taken for instant UV–Vis analysis.

The reaction rate of dye **1** decolorization could be given by the kinetic expression:

$$r = -\frac{dc_d(\text{dye } \mathbf{1})}{dt} = k c(\text{dye } \mathbf{1})^m c(\text{Cl}_2, \text{active})^n c(\text{Cl}^-)^p \quad (4)$$

where k is the rate constant, and m , n and p represent partial reaction orders. By testing the different kinetic models for pseudo- m orders, the best consent was obtained for pseudo-first order.

The apparent decolorization pseudo first-order rate constants for different sodium hydroxide concentrations were determined from the slope of the logarithmic plot of the relative concentration of the dye **1** vs. the electrolysis time, as shown in the insert of Fig. 2, in accordance with the kinetic equation:

$$\ln \frac{c(t)}{c_0} = -k_d t \quad (5)$$

where k_d is the apparent pseudo first-order decolorization rate constant expressed in min⁻¹. For all sodium hydroxide concentrations after 20 min of electrolysis the color removal (CR), defined as:

$$CR = \frac{\left(\frac{c(t)}{c_0} \right)_{t=0} - \left(\frac{c(t)}{c_0} \right)_{t=20\text{min}}}{\left(\frac{c(t)}{c_0} \right)_{t=0}} \times 100 \quad (6)$$

depends on the sodium hydroxide concentration between 21 to 97 %. The values of k_d with the corresponding regression coefficients, and CR are given in Table I.

TABLE I. The influence of the sodium hydroxide concentration on the values of k_d with the corresponding regression coefficients and color removal (CR)

$c(\text{NaOH}) / \text{g dm}^{-3}$	k_d / min^{-1}	R^2	$CR / \%$
0.04	0.221	0.9938	97
0.4	0.0740	0.9871	67
1.0	0.0366	0.9843	33
4.0	0.0171	0.9958	21

As can be seen from Fig. 2 and Table I, an increase in the sodium hydroxide concentration (solution pH) decreased the reaction rate. The changes in the absorption spectra of the dye **1** solution (sodium hydroxide concentration = 1 mM) during the electrochemical decolorization are presented in Fig. 3. Under the basic conditions, dye **1** exhibited a main band with a maximum absorption at 389 nm. The decrease of absorption peak actually indicates a rapid decolorization of the dye over time. After 20 min, almost complete decolorization was observed. The absorption peak observed at 292 nm is attributed to hypochlorite.²⁴

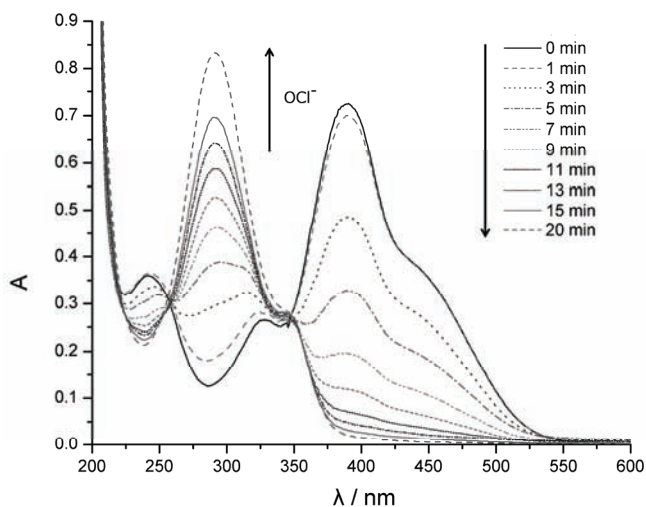


Fig. 3. Changes in the UV–Vis spectrum of dye **1** in water solution ($c(\text{NaOH}) = 1 \text{ mM}$) during electrochemical decolorization. Conditions: $c(\text{dye } \mathbf{1}) = 10 \text{ mg dm}^{-3}$ (30.4 μM), $c(\text{NaCl}) = 20 \text{ g dm}^{-3}$, $\omega = 250 \text{ rpm}$, $I = 200 \text{ mA}$.

The effect of the agitation speed is presented in Fig. 4. The obtained results show a practically negligible effect of the agitation speed on the decolorization of dye **1**. Since the diffusion rate and heterogeneous or homogenous oxidation rate are highly dependent on the hydrodynamic conditions, the only explanation is that the rate determining step is activation controlled (charge transfer) reaction. The only activation controlled reaction could be the oxidation of the chlorides to chlorine given by Eq. (1), followed by fast chlorine disproportionation to HOCl and their dissociation to OCl⁻. In order to resolve which species were active ones, the following experiment was performed: 450 ml of 10 g NaCl was electrolyzed 5 min with 200 mA, and after that a solution of the dye **1** (5 mg in 50 ml of water with 20 mg NaOH) was added. The decolorization occurred practically with an identical rate as during the electrolysis, as can be seen from the inset of Fig. 4. Since pH of the solution was almost constant with a value of ≈ 10 , it could be concluded that hypochlorites were the active species.

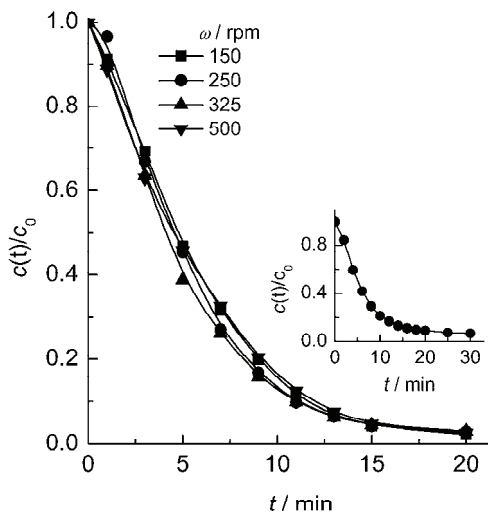


Fig. 4. Dependence of the relative concentration of dye **1** over time for different agitation speeds (marked in the figure). Inset: change of the normalized concentration with time when the dye was added to a hypochlorite solution ($\omega = 325$ rpm).

Effect of the initial sodium chloride concentration

The influence of the sodium chloride concentration on the reaction rate of the decolorization was studied in the range from 15 to 40 g dm⁻³ in solution containing 10 mg dm⁻³ of dye **1**. The sodium hydroxide concentration was 1 mM and applied current 200 mA. As it can be seen, the rate constant increased with increasing salt concentration up to 30 g dm⁻³ (Fig. 5). At higher concentration, namely at 40 g dm⁻³, a small decrease in the reaction rate was observed.

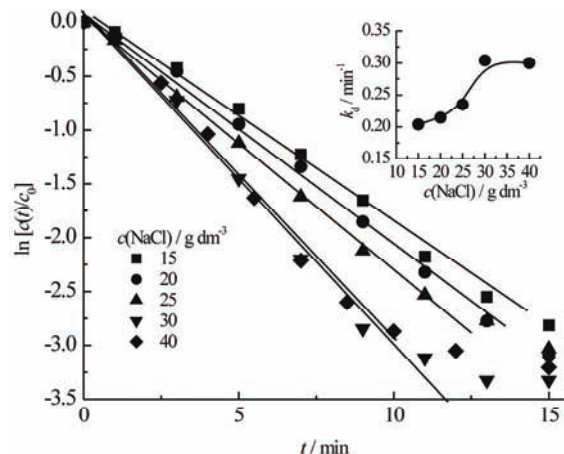


Fig. 5. Dependence of the relative dye **1** concentration over time for different sodium chloride concentrations (marked in the figure). Insert: the reaction rate constant of dye decolorization vs. electrolysis time for the different sodium chloride concentrations. Conditions: $c(\text{dye } \mathbf{1}) = 10 \text{ mg dm}^{-3}$ (30.4 μM), $\omega = 325$ rpm, $c(\text{NaOH}) = 1 \text{ mM}$, $I = 200 \text{ mA}$.

According to the Faraday Law, the amount of the produced hypochlorite should be proportional to the current and the rate should remain constant, *i.e.*, by applying the same current to different solutions, the same amount of hypochlorite should be produced and the rate should be independent (constant) of the elec-

trolyte concentration. One possible explanation is that the production of hypochlorite (Eqs. (1)–(3)) occurs in competition with the production of oxygen:



If this hypothesis is correct, then higher chloride concentrations will increase the percentage proportion of the reaction *via* hypochlorite and decrease the relative production of oxygen.²⁵ This is connected with current efficiency of the hypochlorite production. Namely, as determined by Kraft *et al.*,⁸ in the concentration range of NaCl from 1 to 20 g dm⁻³, the current efficiency of hypochlorite production on a Ti/PtO_x electrode linearly increase from ≈10 to 70 %. Hence, in a solution with a smaller concentration of NaCl, *e.g.*, 15–25 g dm⁻³, the oxygen evolution reaction occurs at the high rate. In a solution with a higher concentration of NaCl, the steady state conditions of current efficiency are reached and the amount of the hypochlorite production becomes constant. Based on this data, the optimum concentration of NaCl would be ≈30 g dm⁻³. However, due to economic and environmental reasons, a sodium chloride concentration of 20 g dm⁻³ was used for the further experiments.

Effect of the initial dye concentration

The next step in this study was to investigate the influence of the initial dye concentration (dye **1**) on the decolorization reaction rate. This investigation was realized using a sodium chloride concentration of 20 g dm⁻³, an applied current of 200 mA and an agitation speed of 325 rpm. The effect of different initial dye concentrations (5–20 mg dm⁻³) on the decolorization rate of dye **1** is displayed in Fig. 6. As can be seen from Fig. 6, and from the inset of Fig. 6, increasing the dye concentration decreased the reaction rate, while above a concentration of 20 mg dm⁻³, there was a small decrease in the electrocatalytic rate of the decolorization.

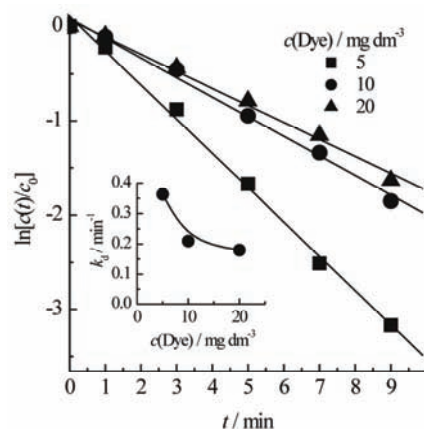


Fig. 6. Dependence of the relative concentration of dye **1** over time for the different dye concentrations (marked in the figure). Insert: the reaction rate constant of dye decolorization vs. electrolysis time for the different dye concentrations. Conditions: $c(\text{NaCl}) = 20 \text{ g dm}^{-3}$, $\omega = 325 \text{ rpm}$, 1 mM NaOH, $I = 200 \text{ mA}$.

Effect of applied current and pH

Applied current is an important variable in electrochemical engineering. Different current values (100, 120, 200 and 250 mA) were applied to the cell in order to investigate the influence of applied current on the electrochemical decolorization of dye **1** a sodium chloride concentration of 20 g dm⁻³ and a dye concentration of 10 mg dm⁻³. Figure 7 shows the dependence of the relative dye **1** concentration over time and the decolorization kinetic rate constants for different values of applied current are shown in Fig. 7. As can be seen, the rate constant, $\approx 0.21 \text{ min}^{-1}$, was partially independent of the applied current in the range from 100 to 200 mA. Above 200 mA, the rate constant deviated from the linearity, probably due to direct oxidation of the dye on the electrode surface.²⁶ Therefore, the current for the further electrochemical studies was fixed at 200 mA.

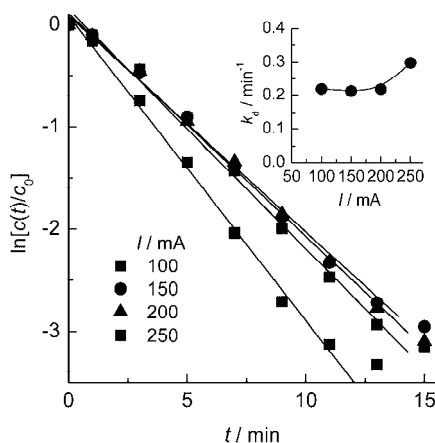


Fig. 7. Dependence of the relative concentration of dye **1** over time for the different values of the applied current (marked in the figure). Inset: the reaction rate constant of dye decolorization vs. electrolysis time for different values of the applied current. Conditions: $c(\text{dye } \mathbf{1}) = 10 \text{ mg dm}^{-3}$ (30.4 μM), $c(\text{NaCl}) = 20 \text{ g dm}^{-3}$, $\omega = 325 \text{ rpm}$, 1 mM NaOH.

In addition, the pH value of the reaction mixture was measured during the electrolysis of dye **1**. As mentioned before, due to the low solubility of arylazo pyridone dyes, the reactions were performed under basic conditions. It was shown earlier that an increase of pH is evident during electrochemical decolorization.²³ The increase in the solution pH decreases the reaction rate, which could be connected with the dissociation of hypochlorous acid to hypochlorite. Here, the initial pH was 10.3 and there was almost no change in the pH value during the reaction. The increase in the hypochlorite concentration is evident from UV–Vis spectra, as shown in Fig. 3.

Influence of the dye structure

It is well known that arylazo pyridone dyes exhibit azo–hydrazone tautomerism, which is presented in Fig. 8.^{27,28} Structure (1) presents the azo tautomer, while structure (4) presents the hydrazone tautomer. Under the basic conditions, they form the azo (2) and hydrazone anion (3), which are resonance hybrids.

Generally, arylazo pyridone dyes exist in the hydrazone form in the solid state, while in solvents, depending on the dye structure and the solvent used, the azo–hydrazone equilibrium exists.^{16,27} Under basic conditions, depending on the substituent in the aryl component of dye, the dye exists mainly as the azo or hydrazone anion. As it can be seen from Fig. 3, the main absorption peak for dye **1** was at 389 nm, which corresponds to the azo anion structure. The shoulder observed at \approx 470 nm is ascribed to the hydrazone form. The same pattern was observed for other dyes (Fig. 9), except for dye **2**, which exhibited a distinguished peak for the hydrazone form at 460 nm.

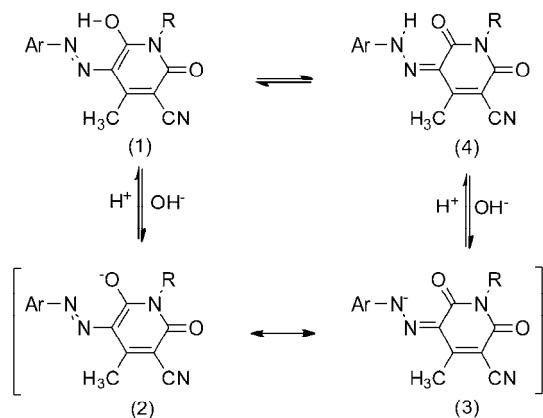


Fig. 8. Azo–hydrazone tautomerism in the arylazo pyridone dyes (azo tautomer (1), azo anion (2), hydrazone anion (3) and hydrazone tautomer (4)).

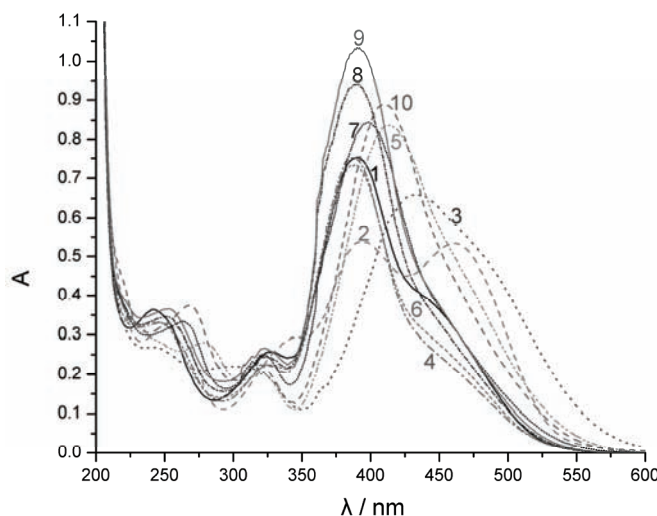


Fig. 9. UV–Vis spectra of the dyes (5-(4-substituted-phenylazo)-3-cyano-1-(2-hydroxyethyl)-6-hydroxy-4-methyl-2-pyridones (**1–10**) in water solutions (1 mM NaOH).

In order to obtain more information on the reaction mechanism, a series of 5-(4-substituted-phenylazo)-3-cyano-1-(2-hydroxyethyl)-6-hydroxy-4-methyl-2-pyridones (**1–10**) were subjected to electrochemical decolorization under the following conditions: dye concentration = 30.4 µM, sodium chloride concentration = 20 g dm⁻³, agitation speed = 325 rpm, sodium hydroxide concentration = 1 mM and current = 200 mA. A lower sodium chloride concentration was selected in order to obtain slower reactions, which made the experimental work (UV–Vis handling) easier. The obtained results are presented in Table II.

The effects of the substituents in the investigated compounds were interpreted by correlation of the reaction rate constants with the Hammett substituent constants σ_p/σ_{p^-} where σ_p/σ_{p^-} measures the electronic effect of the substituent in the *para* position.^{31,32}

TABLE II. Substituent effect on the electrochemical decolorization of 5-(4-substituted-phenylazo)-3-cyano-1-(2-hydroxyethyl)-6-hydroxy-4-methyl-2-pyridones (**1–10**)

Dye	X	$\lambda_{\text{max}} / \text{nm}$	$k_{\text{app}} / \text{min}^{-1}$	σ_p/σ_{p^-}
1	OCH ₃	389	0.221	-0.28 ³¹
2	O ⁻	460	0.3557	-2.30 ³²
3	NO ₂	434	0.1233	1.27 ³¹
4	H	388	0.21	0.00 ³¹
5	CH ₃ CO	412	0.171	0.47 ³¹
6	CH ₃	389	0.234	-0.14 ³¹
7	COO ⁻	398	0.3463	0.31 ³²
8	Cl	390	0.2724	0.24 ³¹
9	Br	390	0.2847	0.26 ³¹
10	CN	411	0.158	1.00 ³¹

A better correlation of the reaction rate constants was obtained with the σ_p -constants for electron-accepting substituents, than with the σ_p constants (excluding Cl, Br and COO⁻ groups as substituents with negative inductive and positive resonance effects), which indicates extensive delocalization of the negative charge on the reaction center. The correlation presented in Fig. 10 is interpreted as the existence of the hydrazone anion in the transition state of this reaction. Electron-accepting substituents inhibit the reaction, while electron-donating substituents promote the reaction.

In addition, dye **11** was decolorized under the same conditions as given in Table II, in order to determine the effect of a substituent in position 1 of the 2-pyridone ring. Dye **12** was partially soluble in the aqueous sodium hydroxide water at a concentration of 1 mM and so only the reaction with dye **11** was achieved. The obtained results are given in Fig. 11, indicating that group in position 1 of the pyridone ring has negligible influence on the reaction rate. This indicates that the substituents on the phenyl ring have more influence on the reaction center during the electrochemical decolorization of the dyes.

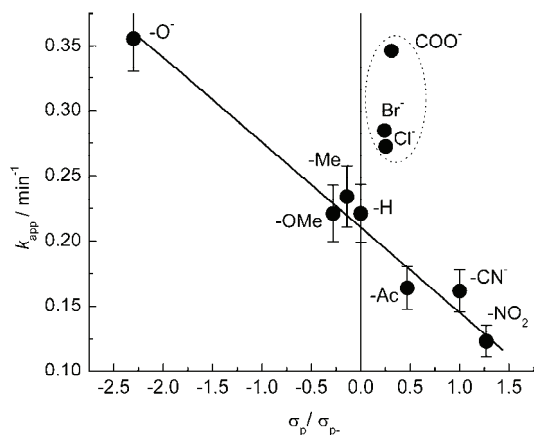


Fig. 10. Relationship between k_{app} and σ_p/σ_{p^-} for arylazo pyridone dyes **1–10**.

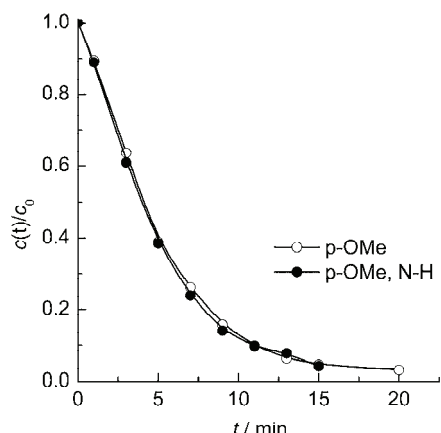


Fig. 11. Dependence of the relative dye concentration over time for dyes **1** and **11**. Conditions: $c(\text{dye}) = 10 \text{ mg dm}^{-3}$ ($30.4 \mu\text{M}$), $c(\text{NaCl}) = 20 \text{ g dm}^{-3}$, $\omega = 325 \text{ rpm}$, 1 mM NaOH , $I = 200 \text{ mA}$.

According to Kanazawa and Onami, the conversion of the hydrazone tautomer (here anion) to hydrazone chloride ($\text{N}(\text{Cl})-\text{N}=$) is considered to be the rate determining step of the reaction.³³ Moreover, Omura suggested that the electrophilic attack of the chloronium ion (Cl^+) on the nitrogen atom in the hydrazone tautomer of azo dyes is a rate-determining step and because of that the degradation rate of the azo dyes depends on the first power of the dye concentration.³⁴ Thus, the hydrazone anion would be attacked by chloronium ion. Then OCl^- attacks the imino group of hydrazone chloride giving a single bond between two nitrogens and thus producing the decolorization of an azo dye. Since it was suggested that the rate-determining step is the electrophilic attack of the chloronium ion on the nitrogen atom of the hydrazone anion, it is clear why electron-accepting substituents retard the reaction, while electron-donating substituents promote the reaction. The electron-donating substituents promote the

reaction by increasing the electron density on the nitrogen atom of the hydrazone anion, thus lowering the energy barrier for the electrophilic attack.

CONCLUSIONS

Based on the presented data, the following could be evaluated. The agitation speed between 150 and 500 rpm had a negligible effect of on the decolorization rate. The rate constant increased with increasing salt concentration up to 30 g dm⁻³. At a higher concentration, namely at 40 g dm⁻³, a small decrease in the reaction rate was observed. Increasing the dye concentration decreased the reaction rate, up to concentration of 10 mg dm⁻³, above which there was a small, almost negligible decrease in the electrocatalytic rate of decolorization. Above 200 mA, the rate constant deviated from linearity, probably due to the direct oxidation of the dye on the electrode surface. The optimum electrolyte should contain \approx 30 g dm⁻³ NaCl, and the current should be 200 mA (400 mA dm⁻²). It could also be concluded that electron-accepting substituents inhibited the reaction, while electron-donating substituents promoted the reaction. Electron-donating substituents promoted the reaction by increasing the electron density on the nitrogen atom of the hydrazone anion thus lowering the energy barrier for the electrophilic attack by chloronium ion.

SUPPLEMENTARY MATERIAL

Physical, analytic and spectral data for the synthesized dyes are available electronically from <http://www.shd.org.rs/JSCS/>, or from the corresponding author on request.

Acknowledgement. The work was supported by the Ministry of Education, Science and Technological Development of the Republic of Serbia under the Research Projects Nos. OI172013 and OI172046.

ИЗВОД

ОПТИМИЗАЦИЈА ЕЛЕКТРОХЕМИЈСКОГ ОБЕЗБОЈАВАЊА ОДРЕЂЕНИХ АРИЛАЗО ПИРИДОНСКИХ БОЈА

ЈЕЛЕНА М. МИРКОВИЋ, НЕВЕНА Ж. ПРЛАИНОВИЋ, ГОРДАНА С. УШЋУМЛИЋ, БРАНИМИР Н. ГРГУР и ДУШАН Ж. МИЈИН

Технолошко-мештаварски факултет, Универзитет у Београду, Карнеијева 4, 11020 Београд

Електрокаталитичко обезбојавање арилазо пиридонских боја испитивано је у присуству натријум-хлорида у разблаженом раствору натријум-хидроксида користећи DSA Ti/PtO_x електроду. Обезбојавање се може приписати индиректној оксидацији испитиваних боја помоћу хипохлорита насталог електрохемијском оксидацијом хлорида. Процес обезбојавања је испитиван варирањем концентрације натријум-хидроксида у опсегу од 40 mg dm⁻³ до 4 g dm⁻³, концентрације натријум-хлорида од 15 до 40 g dm⁻³, јачине струје од 100 до 250 mA и концентрације боје од 5 до 20 mg dm⁻³. На основу добијених резултата утврђени су оптимални услови електролизе. Поред тога, испитиван је и утицај супституената на брзину електрохемијског обезбојавања арилазо пиридонских боја.

(Примљено 9. априла, ревидирано 30. маја, прихваћено 18. јуна 2014)

REFERENCES

1. H. Zollinger, *Colour Chemistry*, Wiley–VCH, Weinheim, 1987, p. 85
2. R. J. Chudgar, J. Oakes, in *Kirk-Othmer Encyclopedia of Chemical Technology*, Wiley, New York, 2003, doi: 10.1002/0471238961.01261503082104.a01.pub2
3. E. Foracs, T. Cserhati, G. Oros, *Environ. Int.* **30** (2004) 953
4. I. K. Konstantinou, T. A. Albanis, *Appl. Cat., B* **49** (2004) 1
5. Y. M. Slokar, A. M. Le Marechal, *Dyes Pigm.* **37** (1998) 335
6. A. H. Konsowa, *Desalination* **158** (2003) 233
7. C. A. Martinez-Huitle, E. Brillas, *Appl. Cat., B* **87** (2009) 105
8. A. Kraft, M. Stadelmann, M. Blaschke, D. Kreysig, B. Sandt, F. Schroéder, J. Rennau, *J. Appl. Electrochem.* **29** (1999) 861
9. I. J. Wang, P. Y. Wang, *Text. Res. J.* **60** (1990) 297
10. P. Y. Wang, I. J. Wang, *Text. Res. J.* **60** (1990) 519
11. P. Y. Wang, I. J. Wang, *Text. Res. J.* **61** (1991) 162
12. P. Y. Wang, I. J. Wang, *Text. Res. J.* **62** (1992) 15
13. J. M. Dostanić, D. R. Lončarević, P. T. Banković, O. G. Cvetković, D. M. Jovanović, D. Ž. Mijin, *J. Environ. Sci. Heal., A* **46** (2011) 70
14. J. M. Dostanić, D. R. Lončarević, Lj. S. Rozić, S. P. Petrović, D. Ž. Mijin, D. M. Jovanović, *Desalin. Water Treat.* **51** (2013) 2802
15. L. Szpyrkowicz, C. Juzzolino, S. N. Kaul, *Water Res.* **35** (2001) 2129
16. N. Ertan, P. Gurkan, *Dyes Pigm.* **33** (1997) 137
17. J. M. Bobbit, D. A. Scola, *J. Org. Chem.* **25** (1960) 560
18. D. Ž. Mijin, B. D. Milić, M. M. Mišić-Vuković, *Indian J. Chem., B* **45** (2006) 993
19. C. C. Chen, I. J. Wang, *Dyes Pigm.* **15** (1991) 69
20. Q. Peng, M. Li, K. Gao, L. Cheng, *Dyes Pigm.* **18** (1992) 271
21. J. Dostanić, N. Valentić, G. Ušćumlić, D. Mijin, *J. Serb. Chem. Soc.* **76** (2011) 499
22. J. Mirković, J. Rogan, D. Poleti, V. Vitnik, Ž. Vitnik, G. Ušćumlić, D. Mijin, *Dyes Pigm.* **104** (2014) 160
23. D. Ž. Mijin, M. L. Avramov Ivić, A. E. Onjia, B. N. Grgur, *Chem. Eng. J.* **204–206** (2012) 151
24. L. C. Adam, I. Fábián, K. Suzuki, G. Gordon, *Inorg. Chem.* **31** (1992) 3534
25. J. P. Lorimer, T. J. Mason, M. Plattes, S. S. Phull, D. J. Walton, *Pure Appl. Chem.* **73** (2001) 1957
26. H. S. Awad, N. Abo Galwa, *Chemosphere* **61** (2005) 1327
27. G. S. Ušćumlić, D. Ž. Mijin, V. V. Vajs, B. M. Sušić, *Chem. Phys. Lett.* **397** (2004) 148
28. A. Alimmarri, D. Mijin, R. Vukićević, B. Božić, N. Valentić, V. Vitnik, Ž. Vitnik, G. Ušćumlić, *Chem. Cent. J.* **6** (2012) 1
29. M. B. Smith, J. March, *March's Advanced Organic Chemistry - Reactions, Mechanisms, and Structure*, Wiley, Hoboken, NJ, 2007, p. 404
30. H. Corwin, A. Leo, R. W. Taft, *Chem. Rev.* **97** (1991) 165
31. L. P. Hammett, *J. Am. Chem. Soc.* **59** (1937) 96
32. M. Charton, *Prog. Phys. Org. Chem.* **13** (1981) 119
33. H. Kanazawa, T. Onami, *Color. Technol.* **117** (2001) 323
34. T. Omura, *Dyes Pigm.* **26** (1994) 33.